

Chapter 3

The User's Role in Haptic System Design

Thorsten A. Kern and Christian Hatzfeld

Abstract A good mechanical design has to consider the user in his or her mechanical properties. The first part of this chapter deals with the discussion of the user as a mechanical *load* on the haptic device. The corresponding model is split into two independent elements depending on the frequency range of the oscillation. Methods and measurement setups for the derivation of mechanical impedance of the user are reviewed, and a thorough analysis of impedance for different grip configurations is presented. In the second part of the chapter, the user is considered as the ultimate measure of quality for a haptic system. The relation of psychophysical parameters like the absolute threshold or the JND to engineering quality measures like resolution, errors, and reproducibility is described and application depending quality measures like haptic transparency are introduced.

3.1 The User as Mechanical Load

Thorsten A. Kern

3.1.1 Mapping of Frequency Ranges onto the User's Mechanical Model

The area of active haptic interaction movements—made in a conscious and controlled way by the user—is of limited range. Sources concerning the dynamics of human movements differ as outlined in the preceding chapters. The fastest conscious move-

T.A. Kern (✉)
Continental Automotive GmbH, VDO-Straße 1, 64832 Babenhausen, Germany
e-mail: t.kern@hapticdevices.eu

C. Hatzfeld
Institute of Electromechanical Design, Technische Universität Darmstadt,
Merckstr. 25, 64283 Darmstadt, Germany
e-mail: c.hatzfeld@hapticdevices.eu

© Springer-Verlag London 2014
C. Hatzfeld and T.A. Kern (eds.), *Engineering Haptic Devices*,
Springer Series on Touch and Haptic Systems, DOI 10.1007/978-1-4471-6518-7_3

ment performed by humans is done with the fingers. Movements for typing of up to 8 Hz can be observed.¹ As these values refer to a ten-finger interaction, they have to be modified slightly. However, as the border frequency of a movement lies above the pure number of a repetitive event, an assumption of the upper border frequency of 10 Hz for active, controlled movement covers most cases.

The major part of the spectrum of haptic perception is passive (*passive haptic interaction*, see Fig. 1.7). The user does not have any active influence or feedback within this passive frequency range. In fact, the user is able to modify his properties as a mechanical load by altering the force when holding a knob. But although this change influences the higher frequency range, the change itself happens with lower dynamics within the dynamic range of active haptic interaction. A look at haptic systems addressing tactile and kinaesthetic interaction channels shows that the above modeling has slightly different impacts:

- The output values of kinaesthetic systems F_{out} (Fig. 3.1a) result in two reactions by the user. First, a spontaneous, not directly controllable movement reaction v_{spo} happens as a result of the mechanical properties of the fingertip (depending on the type of grasp, this can be also the complete interior hand and its skin elasticity). Second, an additional perception of forces takes place. This perception K^2 is weighted according to the actual situation and results in a conscious reaction of the motor parts of the body. These induced reactions v_{ind} summed up with the spontaneous reactions result in the combined output value v_{out} of the user.
- The movements of tactile devices v_{out} (Fig. 3.1b) and the consciously performed movement of the user v_{ind} result in a combined movement and velocity. This elongation acts on the skin, generating the output value F_{out} as a result of its mechanical properties. This conscious movement v_{ind} sums up to v_{out} in the opposite direction of the original movement, as with opposite movement directions, the skin's elongation increases and results in a larger force between user and technical system. Analogously, it subtracts with movements in the same direction, as in this case, the device (or the user, depending on the point of view) evades the acting force trying to keep deformation low and to perceive just a small haptic feedback. According to this model, only the output value F_{out} of the combined movement is perceived and contributes to a willingly induced movement.

If you transfer the model of Fig. 3.1 into an abstract notation, all blocks correspond to the transfer function G_{Hn} . Additionally, it has to be considered that the user's reaction K' is a combined reaction of complex habits and the perception K ; therefore, a necessity to simplify this branch of the model becomes eminent. For the purpose of device design and requirement specification, the conscious reaction is modeled by a disturbing variable only limited in bandwidth, resulting in a block diagram

¹ 8 Hz corresponds to a typing speed of 480 keystrokes per minute. Four hundred keystrokes are regarded as very good for a professional typist, 300–200 keystrokes are good, and 100 keystrokes can be achieved by most laymen.

² K , a variable chosen completely arbitrarily, is a helpful construct for understanding block diagrams rather than having a real neurological analogy.

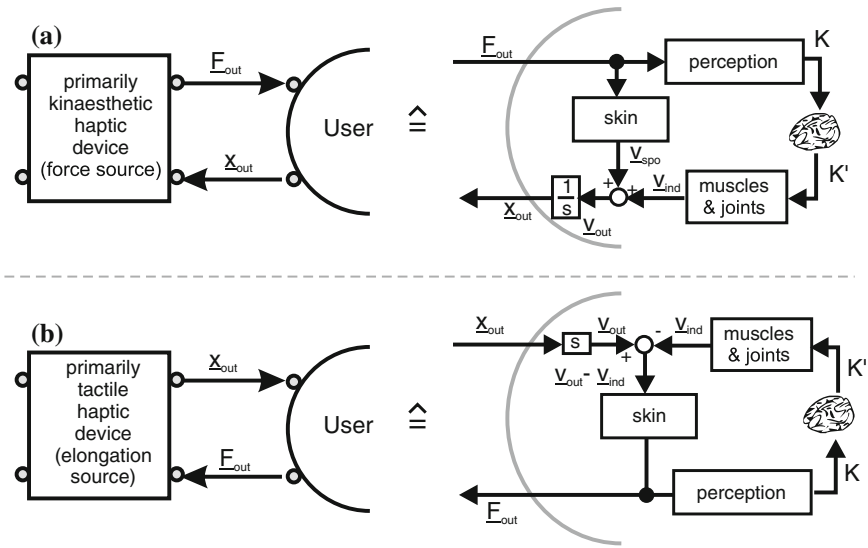


Fig. 3.1 User models as a block structure from kinaesthetic (a) and tactile (b) systems

according to Fig. 3.2c for kinaesthetic and according to Fig. 3.2d for tactile devices. The transfer function G_{H3} corresponds to the mechanical admittance of the grasp above the border frequency of user interaction f_g .

With regard to the application of the presented models, there are two remarks to be considered:

- The notation in Figs. 3.1 and 3.2 for elongations x and forces F being input and output values of users is just one approach to the description. In fact, an *impedance coupling* exists between user and haptic system, making it impossible to distinguish between input and output parameters. However, the decoupled haptic device is designed for being a position or force source. This in fact is the major motivation to define input and/or output parameters of the user. But there are certain actuators (e.g., ultrasonic devices) which can hardly be defined as being part of either one of these classes. As a consequence, when describing either system, the choice of the leading sign and the direction of arrows should carefully be done!
- The major motivation for this model is the description of a mechanical load for the optimized dimensioning of a haptic system. To guarantee the closed-loop control engineering stability of a simulation or a telemanipulation system, further care has to be taken of the frequency range of active haptic interaction below 10 Hz. Stability analysis in this area can either be achieved by more detailed models or by an observation of input and output values according to their *control engineering passivity*. Further information on this topic can be found in Chap. 7.

The following sections on user impedance give a practical model for the transfer function G_{H3} used in Fig. 3.2.

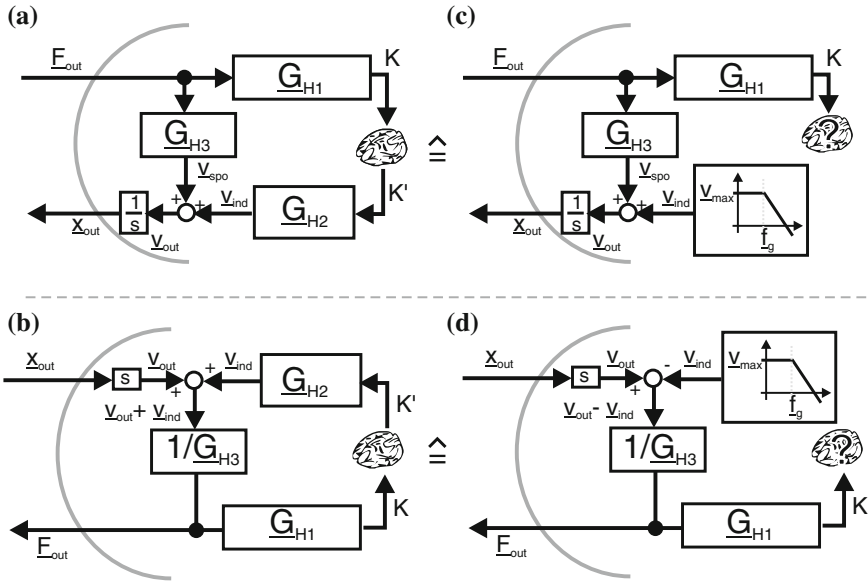


Fig. 3.2 Transformation of the user models’ block structures in transfer functions including simplifications of the model for the area of active haptic interaction for kinaesthetic (a + c) and tactile (b + d) systems

3.1.2 Modeling the Mechanical Impedance

The user’s reaction as part of any haptic interaction combines a conscious, bandwidth-limited portion—the area of active haptic interaction—and a passive portion, mainly resulting from the mechanical properties of fingers, skin, and bones. The influence of this second part stretches across the whole frequency range, but emphasizes the upper area for high frequencies. This section describes the passive part of haptic interaction. The transfer function G_{H3} as in Fig. 3.2 is a component of the impedance coupling with force-input and velocity-output and is therefore a mechanical admittance of the human Y_H respectively the mechanical impedance Z_H .

$$G_{H3} = \frac{v_{spo}}{F_{out}} = \frac{v_{out} - v_{ind}}{F_{out}} = Y_H = \frac{1}{Z_H} \tag{3.1}$$

In the following, this mechanical impedance of the user is specified. The parameter impedance combines all mechanical parameters of an object or system that can be expressed in a linear, time-invariant description, i.e., mass m , compliance k , and damping d . High impedance therefore means that an object has at least one of the three properties:

1. hard and stiff in the sense of spring stiffness,
2. large mass in the sense of inertial force,
3. sticky and tight in the sense of high friction.

In any case, a small movement (velocity v) results in a high force reaction F with high impedances. Low impedance means that the object, the mechanics, is accordingly soft and light. Even high velocities result in small counter forces in this case. The human mechanical impedance is dependent on a number of influence parameters:

- type of grasp being directly influenced by the construction of the handle,
- physiological condition,
- grasping force being directly influenced by the will of the user,
- skin surface properties, for example, skin moisture.

The quantification of human mechanical impedance requires taking as many aspects into account as possible. The type of grasp is defined by the mechanical design of the device. Nevertheless, a selection of typical grasping situations will give a good overview of typical impedances appearing during human-machine interaction. User-individual parameters like physiological condition and skin structure can be covered best by the analysis of a large number of people of different conditions. By choosing this approach, a span of percentiles can be acquired covering the mechanical impedances typically appearing with human users. The “free will” itself, however, is—similar to the area of active haptic interaction—hard if not impossible to be modeled. The time-dependent and unpredictable user impedance dependency on the will can only be compensated if the system is designed to cover all possible impedance couplings of actively influenced touch. Another approach would be to indirectly measure the will to adapt the impedance model of the user within the control loop. Such an indirect measure is, in many typical grasping situations, the force applied between two fingers or even the whole hand holding an object or a handle. In the simplest design, the acquisition of such a force can be done by a so-called *dead-man-switch*, which in 1988 was proposed by HANNAFORD for use in haptic systems [8]. A dead-man-switch is pressed as long as the user holds the control handle in his or her hand. It detects the release of the handle resulting in a change in impedance from Z_H to 0.

3.1.3 Grips and Grasps

There is a nomenclature for different types of grasps shown in Fig. 3.3. The hand is an extremity with 27 bones and 33 muscles. It combines 13 (fingers), respectively, 15 (incl. the wrist) degrees of freedom.³ Accordingly, the capabilities of man to grasp are extremely versatile.

³ Thumb: 4 DoF, index finger: 3 DoF, middle finger: 2 DoF (sometimes 3 DoF), ring finger: 2 DoF, small finger: 2 DoF, wrist: 2 DoF. The rotation of the whole hand happens in the forearm and therefore does not count among the degrees of freedom of the hand itself.

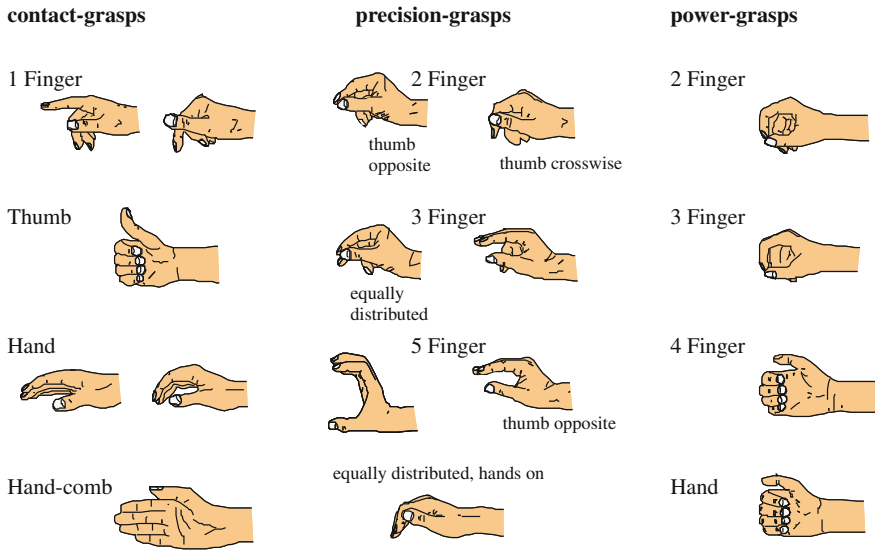


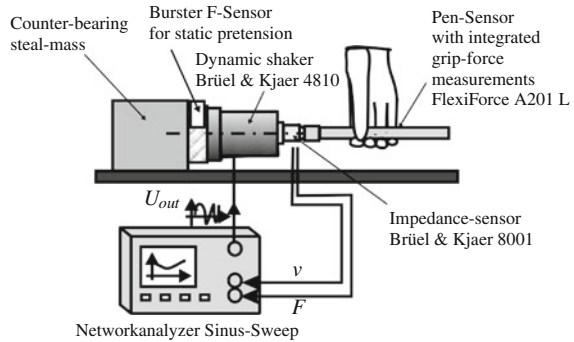
Fig. 3.3 Grip configurations, figure based on [2]

There are three classes of grasps to be distinguished:

- The **contact grasp** describes the touch of an object using the whole hand or major parts of it. Keys and buttons are typically actuated by contact grasps. Even the fingers resting on a keyboard or a piano are called contact grasps. A contact grasp always blocks one direction of movement for an object (which is one half of a degree of freedom). Contact grasps can be regarded as linear only in case of a preload high enough. With light touches, the point of release and the according liftoff of the object are always nonlinear.
- The **precision grasp** describes grasping with several fingers. Typically, a precision grasp locks at least one degree of freedom of the grasped object by form closure with one finger and a counter bearing—often another finger. Additional degrees of freedom are hindered by friction. Precision grasps vary in stiffness of coupling between man and machine. At the same time, they are the most frequent type of grasping.
- The **power grasp** describes an object with at least one finger and a counter bearing, which may be another finger, but is frequently the whole hand. The power grasp aims at locking the grasped object in all degrees of freedom by a combination of form and force closures. Power grasps are—as the name already implies—the stiffest coupling between humans and machines.

Further discrimination of grasps is made by FEIX ET AL. [3] and documented online with the purpose of reducing the mechanical complexity of anthropomorphic hands [4]. The reported taxonomy could be useful for very specialized task-specific

Fig. 3.4 Measurement setup for the acquisition of user impedances according to [16]



systems. For all classes of grasps, measurements of the human's impedance can be performed. According to the approach presented by KERN [16], the measurement method and the models of user impedance are presented including the corresponding model parameters in the following sections.

3.1.4 Measurement Setup and Equipment

The acquisition of mechanical impedances is a well-known problem in measurement technology. The principle of measurement is based on an excitation of the system to be measured by an actuator, simultaneously measuring force and velocity responses of the system. For this purpose, combined force and acceleration sensors (e.g., the impedance sensor 8001 from Brüel & Kjaer, Nærum, DK) exist, whereby the charge amplifier of the acceleration sensor includes an integrator to generate velocity signals.

In [22], WIERTLEWSKI and HAYWARD argue that measurements with impedance heads are prone to measurement errors because of the mechanical construction of the sensor based on BROWNJOHN ET AL. [1]. However, errors induced by the construction of the measurement head appear at frequencies larger than 2,000 Hz, values that are only seldom used in the design of haptic interfaces. Furthermore, interpersonal variations and calibration of the measurement setup based on a concentrated network parameter approach are used to minimize the errors even for high frequencies in the following.

In general, the impedance of organic systems is *nonlinear* and *time variant*. This nonlinearity is a result of a general viscoelastic behavior of tissue resulting from a combined response of relaxation, conditioning, stretching, and creeping [6]. These effects can be reproduced by mechanical models with concentrated elements. However, they are dependent on the time history of excitation to the measured object. It can be expected that measurements based on step excitation are different from those acquired with a sinusoid sweep. Additionally, the absolute time for measurement has some influence on the measures by conditioning. Both effects are systematic mea-

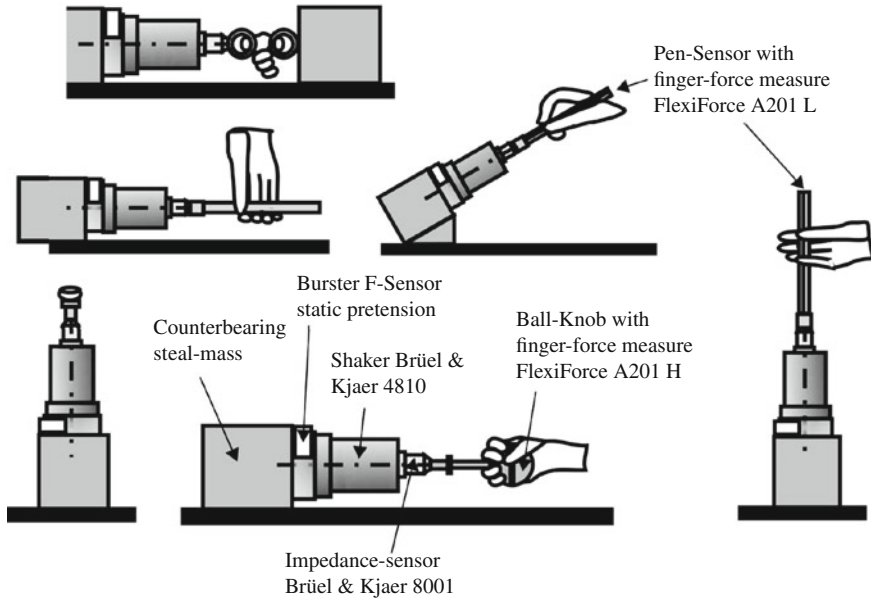


Fig. 3.5 Impedance measurement settings for different grasps

surement errors. Consequently, the models resulting from such measurements are an indication of the technical design process and should always be interpreted with awareness of their variance and errors.

All impedance measures presented here are based on a sinusoid sweep from upper to lower frequencies. The excitation has been made with a defined force of 2N amplitude at the sensor. The mechanical impedance of the handle has been measured by calibration measurements and was subtracted from the measured values. The impedance sensors are limited concerning their dynamic and amplitude resolution, of course. As a consequence, the maximum frequency up to which a model is valid depends on the type of grasp and its handle used during measure. This limitation is a direct result of the amplitude resolution of the sensors and the necessity at high frequencies to have a significant difference between the user's impedance and the handle's impedance for the model to be built on. The presented model parameters are limited to the acquired frequency range and cannot be applied to lower or higher frequencies. The measurement setup is given in Fig. 3.5.

3.1.5 Models

In order to approximate the human impedance, a number of different approaches were taken in the past (Fig. 3.6). For its description, mechanical models based on

concentrated linear elements were chosen. They range from models including active user reactions represented by force sources (Fig. 3.6a), to models with just three elements (Fig. 3.6c) and combined models of different designs. The advantage of a mechanical model compared to a defined transfer function with a certain degree in numerator and denominator results from the possibility of interpreting the elements of the model as being a picture of physical reality. Elasticities and dampers connected in circuit with the exciting force can be interpreted as coupling to the skin. Additionally, the mechanical model creates very high rankings by its interconnected elements which allow much better fit to measurements than free transfer functions.

KERN [16] defined an eight-element model based on the models in Fig. 3.6 for the interpolation of the performed impedance measures. The model can be characterized by three impedance groups typical for many grasping situations:

Z_3 (Eq. 3.4) models the elasticity and damping of the skin being in direct contact with the handle. Z_1 (Eq. 3.2) is the central element of the model and describes the mechanical properties of the dominating body parts—frequently fingers. Z_2 (Eq. 3.3) gives an insight into the mechanical properties of the limbs, frequently hands, and allows to make assumptions about the preloads in the joints in a certain grasping situation.

$$Z_1 = \frac{s^2 m_2 + k_1 + d_1 s}{s} \tag{3.2}$$

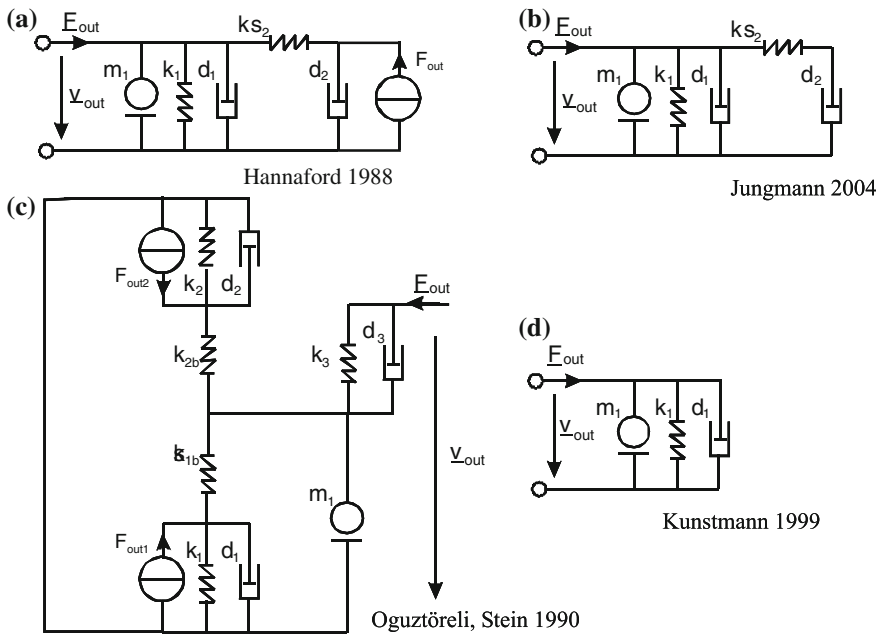


Fig. 3.6 Modeling the user with concentrated elements, a [8], b [15] c [19], d [17]

$$Z_2 = \left(\frac{s}{d_2 s + k_2} + \frac{1}{sm_1} \right)^{-1} \quad (3.3)$$

$$Z_3 = \frac{d_3 s + k_3}{s} \quad (3.4)$$

$$Z_B = Z_1 + Z_2 \quad (3.5)$$

Combined, the model's transformation is given as

$$Z_H = Z_3 \parallel Z_B \quad (3.6)$$

$$Z_H = \left(\frac{s}{d_3 s + k_3} + \left(\frac{s^2 m_2 + k_1 + d_1 s}{s} + \left(\frac{s}{d_2 s + k_2} + \frac{1}{sm_1} \right)^{-1} \right)^{-1} \right)^{-1} \quad (3.7)$$

3.1.6 Modeling Parameters

For the above model (Eq. 3.7), the mechanical parameters can be identified by measurement and approximations with real values. For the values presented here, approximately 48–194 measurements were made. The automated algorithm combines an evolutionary approximation procedure followed by a curve fit with optimization based on Newton curve fitting, to achieve a final adjustment of the evolutionarily found starting parameters according to the measurement data. The measurements vary according to the mechanical preload—the grasping force—to hold and move the control handles. This mechanical preload was measured by force sensors integrated into the handles. For each measurement, this preload could be regarded as being static and was kept by the subjects with a 5% range of the nominal value. As a result, the model's parameters could be quantified not only depending on the grasping situation but also depending on the grasping force. The results are given in the following section. The display of the mechanical impedance is given in decibels, whereby 6 dB equals a doubling of impedance. The list of model values for each grasping situation is given in Appendix A.

3.1.6.1 Power Grasps

Within the class of power grasps, three grasping types were analyzed. Impedance between 35 and 45 dB is measured for the grasp of a cylinder (Fig. 3.8) and of a sphere

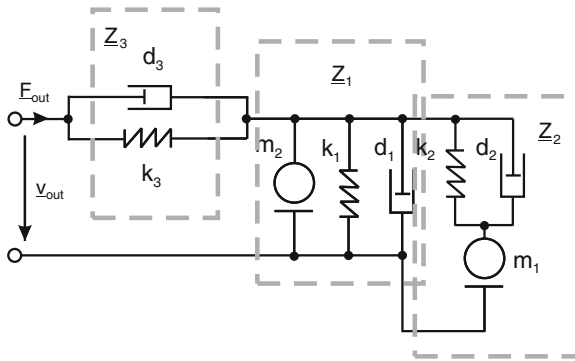


Fig. 3.7 Eight-element model of the user’s impedance [16], modeling the passive mechanics for frequencies >20 Hz

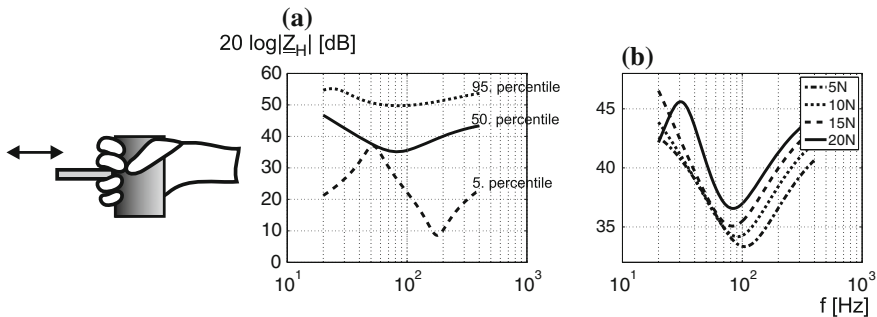


Fig. 3.8 Impedance with percentiles (a) and at different force levels (b) for power grasps of a cylinder (Ø25 mm, defined for 20–400 Hz)

of similar dimensions (Fig. 3.9) with the whole hand. It shows antiresonance in the area of 80 Hz, which moves for a grasp of the cylinder slightly to higher frequencies with increased grasping force. The percentiles, especially the 5th, reveal that the model is based on a large variance and uncertainty. It is likely that the influence of the subjects’ variability in their physical parameters like the size of hands and fingers influences these measurements a great deal.

In case of grasping two rings with thumb and index finger (Fig. 3.10), the results are much more accurate. Impedance ranges between 15 and 35 dB. The antiresonance in the frequency range of 70–100 Hz shows a clear dependency on grasping forces. If we look at the parameters, this change is a result of a variance within the elasticity coefficients k_1 and m_2 , building the central parallel resonance of the model. The mechanical system “hand” becomes stiffer (k_1 increases), but the mass m_2 part of the antiresonance diminishes. An easy interpretation of this effect is not obvious. At a value of 10 kg, the mass m_1 builds an almost stiff counter bearing.

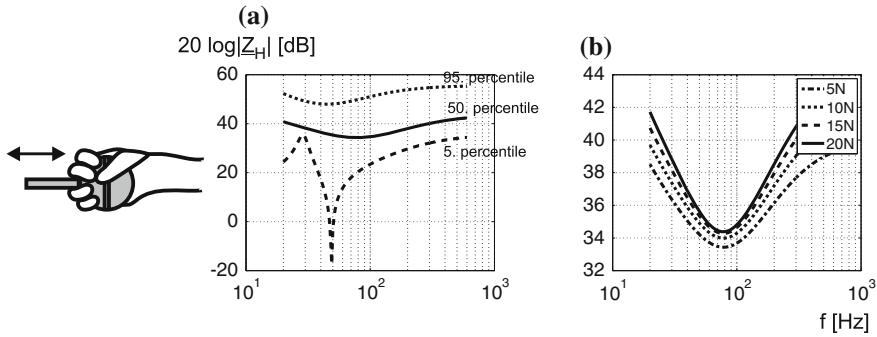


Fig. 3.9 Impedance with percentiles (a) and at different force levels (b) for a power grasp of a sphere ($\text{\O}40$ mm, defined for 20–600 Hz)

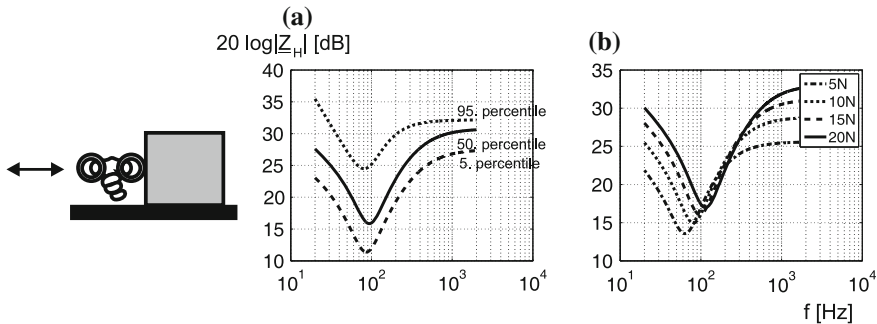


Fig. 3.10 Impedance with percentiles (a) and at different force levels (b) for a two-fingered power grasp of rings ($\text{\O}25$ mm of the inner ring, defined for 20–1 kHz)

3.1.6.2 Precision Grasps

Within the area of precision grasps, three types of grasps were analyzed. Holding a measurement cylinder similar to a normal pen at an angle of 30° (Fig. 3.11), we find a weak antiresonance in the area of around 150–300 Hz. This antiresonance is dependent on the grasping force and moves from weak forces and high frequencies to large forces and lower frequencies. The general dependency makes sense, as the overall system becomes stiffer (the impedance increases) and the coupling between skin and cylinder becomes more efficient resulting in more masses being moved at higher grasping forces.

The general impedance does not change significantly if the cylinder is held in a position similar to a máobi Chinese pen (Fig. 3.12). However, the dependency on the antiresonance slightly diminishes compared to the above pen hold posture.

This is completely different from the variant of a pen in a horizontal position held by a three-finger grasp (Fig. 3.13). A clear antiresonance with frequencies between

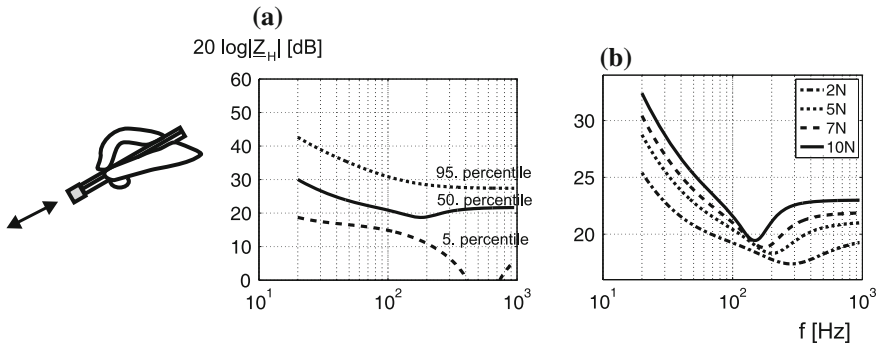


Fig. 3.11 Impedance with percentiles (a) and at different force levels (b) for a two-fingered precision grasp of a pen-like object held like a pen ($\varnothing 10$ mm, defined for 20–950 Hz)

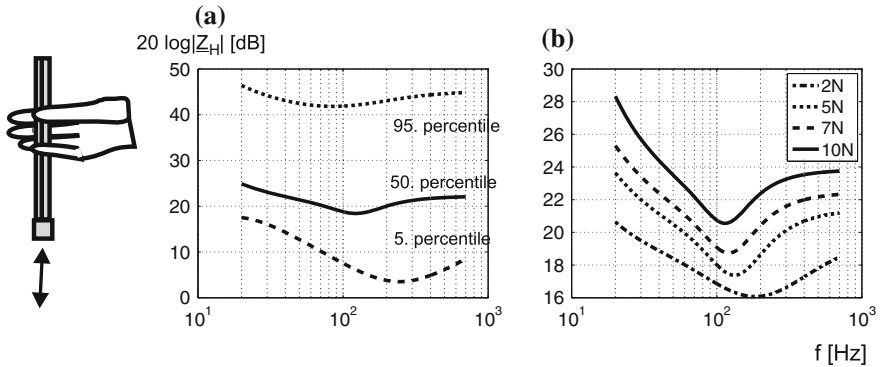


Fig. 3.12 Impedance with percentiles (a) and at different force levels (b) for a two-fingered precision grasp of a pen-like object held like an “máobi” Chinese pen ($\varnothing 10$ mm, defined for 20–700 Hz)

80 and 150 Hz appears largely dependent in shape and position on the grasping force. All observable effects in precision grasps can hardly be traced back to the change of a single parameter but are always a combination of many parameters’ changes.

3.1.6.3 One-Finger Contact Grasp

All measurements were done on the index finger. Direction of touch, size of touched object, and touch force normal to the skin were varied within this analysis. Figure 3.14a shows the overview of the results for a touch being analyzed in normal direction. The mean impedance varies between 10 and 20 dB with a resonance in the range of 100 Hz. Throughout all measured diameters of contactor size and forces, no significant dependency of the position of the antiresonance on touch forces were noted. However, a global increase in impedance is clearly visible. Observing the

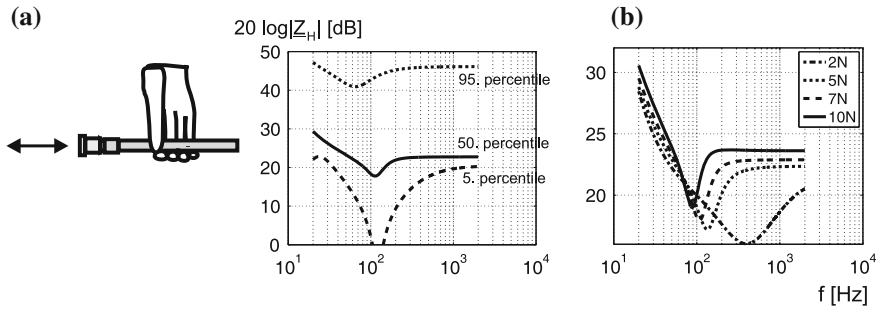


Fig. 3.13 Impedance with percentiles (a) and at different force levels (b) for a five-fingered precision grasp of a pen-like object in horizontal position ($\varnothing 10$ mm, defined for 20–2 kHz)

impedance dependent on contactor size, we can recognize an increase in the antiresonance frequency. Additionally, it is fascinating to see that the stiffness decreases with an increase of contact area. The increase in resonance is probably a result of less material and therefore less inertia participating in generating the impedance. The increase in stiffness may be a result of smaller pins deforming the skin more deeply and therefore getting nearer to the bone as a stiff mechanical counter bearing.

In comparison, with measurements performed with a single pin of only 2 mm in diameter (Fig. 3.14b), the general characteristic of the force dependency can be reproduced. Looking at the largest contact element of 15 mm, in diameter, we are aware of a movement of the resonance frequency from 150 Hz to lower values down to 80 Hz for an increase in contact force.

In orthogonal direction, the skin results differ slightly. Figure 3.15a shows a lateral excitation of the finger pad with an obvious increase of impedance at increased force of touch. This rise is mainly the result of an increase of damping parameters and masses. The position of the antiresonance in frequency domain remains constant at around 150 Hz. The picture changes significantly for the impedance in distal direction (Fig. 3.15b). The impedance still increases, but the resonance moves from high frequencies of around 300 Hz to lower frequencies. Damping increases too, resulting in the antiresonance being diminished until nonexistence. At 45° (Fig. 3.15c), a combination of both effects appears. Antiresonance moves to a higher frequency and loses its sharpness compared to the pure lateral excitation. A first trend of change within the position of the antiresonance in frequency domain with higher forces can be identified additionally.

3.1.6.4 Superordinate Comparison of Grasps

It is interesting to compare the impedances among different types of touch and grasps with each other:

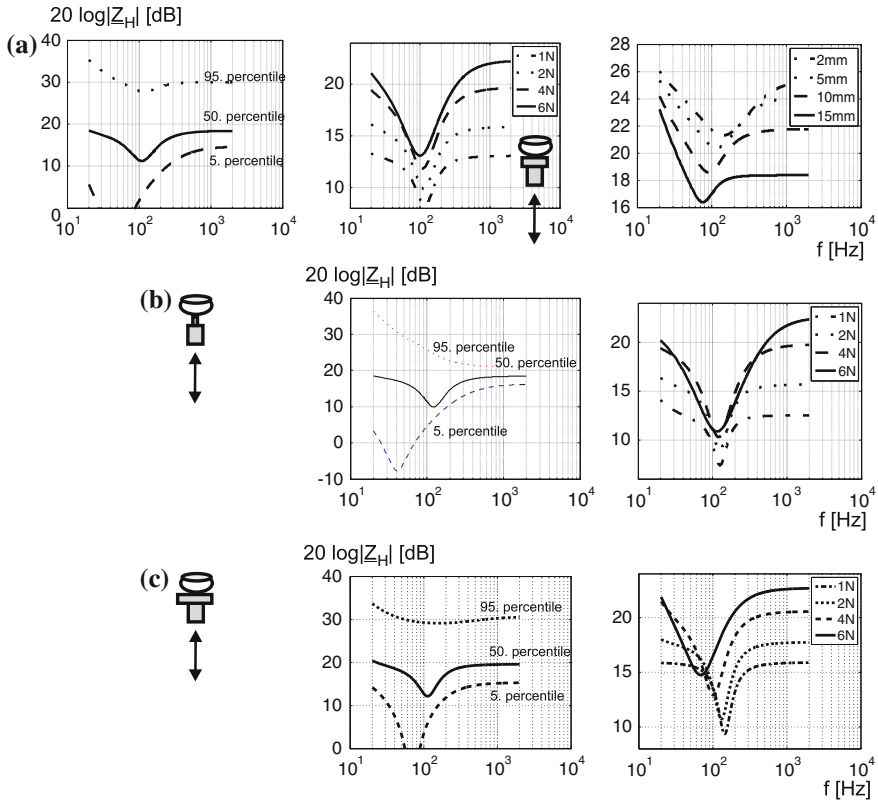


Fig. 3.14 Impedance of finger touch via a *cylindrical plate* for different contact forces (1–6 N) and in dependency from diameter (a), for the *smallest plate* ($\varnothing 2$ mm) (b) and the *largest plate* ($\varnothing 15$ mm) (c) (defined for 20–2 kHz)

- Almost all raw data and the interpolated models show a decrease of impedance within the lower frequency range of 20 Hz to the maximum of the first antiresonance. As for precision grasps (Figs. 3.11, 3.12, 3.13), normal fingertip excitation (Fig. 3.14), and the power grasp of rings (Fig. 3.10), the gradient equals 20 dB/decade resembling a dominating pure elongation proportional effect of force response— elasticity—within a low frequency range. Within this low-bandwidth area, nonlinear effects of tissue including damping seem to be not very relevant. Looking at such interactions, we can assume that any interaction including joint rotation of a finger is almost purely elastic in a low frequency range.
- Many models show clear antiresonance. Its position varies between 70 Hz at power grasps (Figs. 3.8, 3.9, 3.10) and 200 Hz or even 300 Hz at finger touch analyzed in orthogonal direction (Fig. 3.15). The resonance is a natural effect of any system including a mass and elasticity. Therefore, it is not its existence which is relevant for interpretation, but its shape and the position within the frequency range. As to

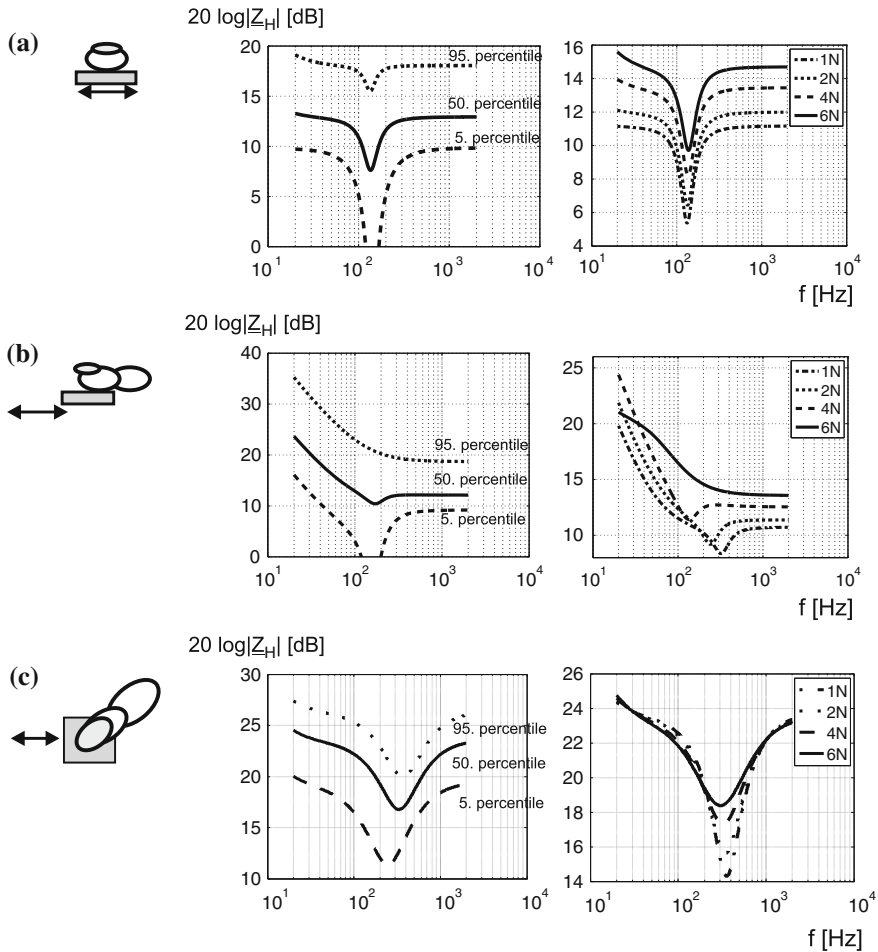


Fig. 3.15 Impedance for finger touch of a plate moving in orthogonal direction to the skin at different force levels (1–6 N) (defined for 20–2 kHz). Movement in lateral direction (a), distal direction (b), and at 45° (c)

positions, especially the power grasp of two rings (Fig. 3.10), the precision grasps of a cylinder in a pen-like position (Fig. 3.11) and in horizontal position (Fig. 3.13) and the touch of an orthogonal moving plate in distal direction (Fig. 3.15c) and a large plate in normal direction (Fig. 3.15c) have a clear dependence on grasping force. The interpretation is not as obvious as in case one. We assume that the normal touch of the plate shows similarities to the contact situation when touching the rings. Additionally, the normal touch is part of the precision grasps mentioned above. In the case of many subjects grasping the horizontal cylinder, it could be observed that the thumb was positioned less orthogonally but more axially to the

cylinder, which could excite it primarily in distal direction, thus also contributing to this effect.

- The shape of the antiresonance is another interesting factor. It can be noted that especially in the analysis of finger grasps and thereat orthogonal excitation (Fig. 3.15a), the antiresonance is very narrow. An interpretation is hard to be formulated. It seems that with grasps and especially touches involving less material the antiresonance becomes narrower in shape.
- For all measurements, at high frequencies above the antiresonance, the frequency characteristic becomes linear and constant, which resembles a pure damping effect. This becomes obvious at the pen-hold posture among the precision grasps (Fig. 3.11) and with the lateral displacement in orthogonal direction, (Fig. 3.15a), but is part of any curve and model. Alternatively, inertia could be assumed to dominate the high frequencies, being represented by a linear increase of mechanical impedance. Mainly, power grasps show a tendency to this increase. This measured effect is especially relevant, as it confirms common assumptions that for high-frequency haptic playback with kinaesthetic devices, the user can be assumed as a damping load.
- A last glance should be taken at the absolute height level and the variance of height of the impedance due to preloads. For all grasps, it varies in a range (regarding the median curves only) of 20 dB as a maximum. Impedance is higher for power grasps, slightly lower for precision grasps, and much lower for touches, which is immediately obvious. The change in the preload for one grasp typically displaces the absolute impedance to higher levels. This displacement varies between 4 and 10 dB.

If speculations should be made on still unknown, not yet analyzed types of touches according to the given data, it should be reasonable to assume the following:

- A. **Power grasp** The median impedance should be around 36 dB. Model the impedance with a dominating elasticity effect until an antiresonance frequency of 80 Hz, not varying much neither in height nor in position of the antiresonance. Afterward, allow inertia to dominate the model's behavior.
- B. **Precision grasp** The median impedance should be around 25 dB. Model the impedance with a dominating elasticity effect until an antiresonance frequency of around 200 Hz. The position of the antiresonance diminishes in an area of 100 Hz due to change in preload. Above that antiresonance, let the impedance become dominated by a damping effect. The height of impedance changes in a range of 5 dB by the force of the grasp.
- C. **Finger touch** The median impedance should be around 12 dB. Model the impedance with a well-balanced elasticity and damping effect until an antiresonance frequency of around 150 Hz. The position of the anti-resonance is constant,

with the exception of large contact areas moving in normal and distal directions. Above that antiresonance, let the impedance become strongly dominated by a damping effect. The absolute height of impedance changes in an area of up to 10dB depending on the force during touch.

3.1.7 Comparison with Existing Models

For further insight into and qualification of the results, a comparison with published mechanical properties of grasps and touches is presented in this section. There are two independent trends of impedance analysis in the scientific focus: the measurement of mechanical impedance as a side product of psychophysical studies at threshold level and measurements at higher impedance levels for general haptic interaction. The frequency plots of models and measurements are shown in Fig. 3.16.

In [11], the force detection thresholds for grasping a pen in normal orientation have been analyzed. Figure 3.16a shows an extract of the results compared to the pen-like grasp of a cylinder of the model in Fig. 3.11 a. Whereas the general level of impedance does fit, the dynamic range covered by our model is not as big as described in the literature. Analyzing the data as published, we can state that the minimum force measured by ISRAR is $\approx 60 \mu\text{N}$ at the point of lowest impedance. A force sensor reliably measuring at this extreme level of sensitivity exceeds the measurement error of our setup and may be the explanation for the difference in the dynamic range

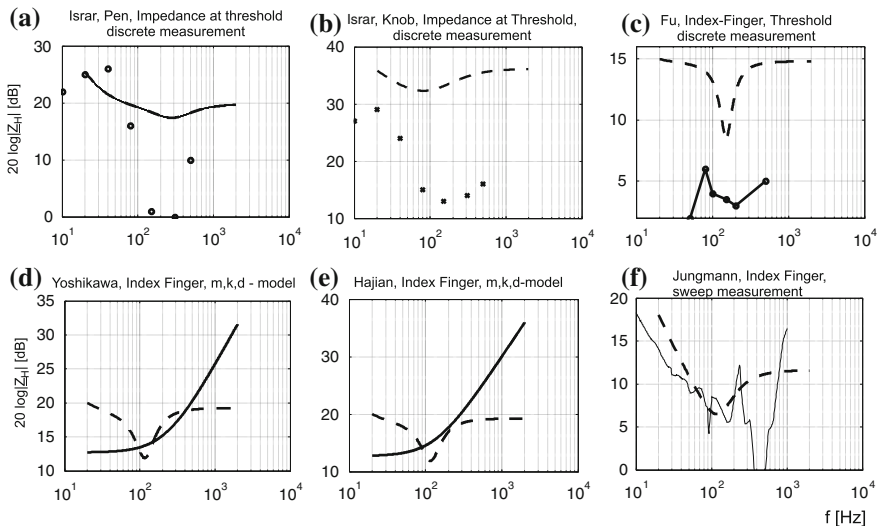


Fig. 3.16 Comparison of the model from Fig. 3.7 with data from similar touches and grasps as published by ISRAR [11, 12], FU [5], YOSHIKAWA [23], HAJIAN [7], JUNGSMANN [14]

covered. In another study [12], the force detection threshold of grasping a sphere with the fingertips was analyzed. The absolute force level of interaction during these measurements was in the range of mN. A comparison (Fig. 3.16b) between our model of touching a sphere and these data show a difference in the range of 10–20 dB. However, such small contact forces resemble a large extrapolation of our model data to low forces. The difference can therefore be easily explained by the error resulting from this extrapolation.

FU [5] measured the impedance of the fingertip at a low force of 0.5 N. He advanced an approach published by HAJIAN [7]. A comparison between our model and their data concerning the shape is hardly possible due to the small number of discrete frequencies of this measurement. However, the impedance is again 10 dB lower than that of our touch model of a 5 mm cylinder at normal oscillations similar to Fig. 3.14. Once more, the literature data describes a level of touch force not covered by our measurements, and therefore, the diagram in Fig. 3.16c is an extrapolation of the model of these low forces.

As a conclusion of this comparison, the model presented here cannot necessarily be applied to measurements done at lower force levels. Publications dealing with touch and grasp at reasonable interaction forces reach nearer to the model parameter estimated by our research. YOSHIKAWA [23] published a study of a three-element mechanical model regarding the index finger. The study was based on a time-domain analysis of a mechanical impact generated by a kinaesthetic haptic device. The measured parameters result in a frequency plot (Fig. 3.16d) which is comparable to our model of low frequencies, but shows neither the complexity nor the variability of our model in a high frequency range of above 100 Hz. A similar study in time domain was performed by HAJIAN [7] with slightly different results. Measurements available as raw data from JUNGSMANN [14] taken in 2002 come close to our results, although obtained with different equipment.

Besides these frequency plots, the model's parameters allow a comparison with absolute values published in the literature: SERINA [21] made a study on the hysteresis of the fingertips' elongation versus force curve during tapping experiments. This study identified a value for k for pulp stiffness ranging from 2 N/mm at a maximum tapping force of 1 N – 7 N/mm at a tapping force of 4 N. This value is about 3–8 times larger than the dominating k_2 in our eight-element model. The results of FU [5] make us assume that there was a systematic error concerning the measurements of SERINA, as the elongation measured at the fingernail does not exclusively correspond to the deformation of the pulp. Therefore, the difference in the values of k between our model and their measurements can become reasonable. Last but not least, MILNER [18] carried out several studies on the mechanical properties of the fingertip in different loading directions. In the relevant loading situation, a value of k ranging from 200 to 500 N/m was identified by him. This is almost perfect within the range of our model's stiffness.

3.1.8 Final Remarks on Impedances

The impedance model as presented here will help in modeling of haptic perception in high frequency ranges above 20 Hz. However, it completely ignores any mechanical properties below this frequency range. This is a direct consequence of the general approach to human-machine interaction presented in Chap. 2 and has to be considered when using this model.

Another aspect to consider is that the above measurements show a large inter-subject variance of impedances. In extreme cases, they span 20 dB meaning nothing else but a factor of 10 between the 5th and the 95th percentiles. Further research on the impedance models will minimize this variance and allow a more precise picture of impedances. But already, this database, although not yet completed, allows to identify helpful trends for human load and haptic devices.

3.2 The User as a Measure of Quality

Christian Hatzfeld

SALISBURY ET AL. postulated a valuable hypothesis for the design of task-specific haptic systems: Their 2011 paper title reads *What You Can't Feel Won't Hurt You: Evaluating Haptic Hardware Using a Haptic Contrast Sensitivity Function* [20]. In this work, they use haptic contrast sensitivity functions (the inverse of the sinusoidal grating detection threshold) to evaluate \leftrightarrow COTS devices. With a more general view, the first part of this paper title summarizes the second role of the user and his or her properties in the design of haptic systems: as the instance that determines whether the presented haptic feedback is good enough or not. In this section, this approach is detailed on three aspects of the system design, i.e., resolutions, errors, and the quality of the haptic interaction.

3.2.1 Resolution of Haptic Systems

Resolution is mainly an issue in the selection and design of sensors and actuators, while the latter is also influenced by the kinematic structure used in interfaces and manipulators. In general, sensors on the manipulation side have so sense at least as good as the human user is able to perceive after the information is haptically displayed by the haptic interface. On the interface side, sensors have to be at least as accurate as the reproducibility of the human motor capability, to convey the users' intention correctly. For the actuating part, the attribution is vice versa: Actuators on the manipulating side have to be as accurate as the human motor capability, while the haptic interface has to be as accurate as human perception can resolve.

Unfortunately, this is the worst case for technical development: Sensors (on the manipulating side) and actuators (on the interfacing side) have to be as accurate as human perception. Therefore, accurate readings of *absolute thresholds* are indispensable to determine the necessary resolutions for sensors and actuators, if one wants to build a high-fidelity haptic system. On the other hand, systematic provisions to alter the perception thresholds favorably by changing the contact situation (contact area, contact forces) at the primary interface are possible. This is further detailed in Sect. 5.2.

For applications not involving teleoperation, the requirements are basically the same, but extend to other parts of the system: For interaction with virtual realities, the software has to supply sufficient discretization of the virtual data (a nontrivial problem, especially if small movements and hard contacts are to be simulated), systems for communication have to supply enough mechanical energy that the perception threshold is surpassed to ensure clear transmission of information. Last but definitely not the least, all errors resulting from digital quantization and other system-inherent noise have to be lower than the absolute perception thresholds of the human user.

3.2.2 Errors and Reproducibility

While resolutions are quite a challenge for the design of haptic systems because of the high sensitivity of human haptic perception, the handling of errors is somewhat easier. The basic assumption about the perception of haptic signals with regard to errors and reproducibility is the following: There is no error if there is no difference detectable by the user. This property is expressed by the \Leftrightarrow JND. *Weber's Law* as stated in Eq. (2.5) facilitates this further: For low references, the acceptable error increases due to increasing differential thresholds. This accommodates the fact that the errors of technical systems and components mainly increase when the reference values decrease.

For large reference values, this relative resolution of human perception is much smaller than the absolute resolution of technical systems that are uniformly distributed along the whole nominal range. This has to be taken into account if information is to be conveyed haptically.

3.2.3 Quality of Haptic Interaction

While resolution and errors are pretty much linked directly to perception parameters, the assessment of haptic quality is somewhat more difficult. It is also based on the assumption that the quality of a haptic interaction is good enough if all intended information is transmitted correctly to the user and no additional information or errors are perceived. The second part can basically be achieved by considering the above-mentioned points regarding errors and resolution. The assessment, whether all information are transmitted correctly, is more difficult since the user and the perceived information have to be taken into account. In general, this is only possible

if suitable evaluation methods are used; Chap. 13 gives an overview of such methods with respect to the intended application.

Another example for the evaluation of haptic quality is the concept of haptic transparency for teleoperation systems. This property describes the ability of a haptic system to convey only the intended information (normally defined as the mechanical impedance of the environment at the manipulator side \underline{Z}_e) to the user (in terms of the displayed impedance of the haptic interface \underline{Z}_t) without displaying the inherent properties of the haptic system. This definition is further detailed in Sect. 7.4.2. Despite the above said, this property can be tested without a user test, but with considerable effort regarding the mechanical measurement setup.

When further considering haptic perception properties, especially \leftrightarrow just noticeable differences, the common binary definition of transparency can be transformed into a nominal value with a lot less requirements on the technical system. This concept was developed by HATZFELD, KASSNER, and NEUPERT [9, 10] and is further explained in Sect. 7.4.2.

One should keep in mind that all of the above-mentioned thresholds are generally dependent on frequency and the contact situation in the best case. In the worst case, they are also dependent on the experimental methodology used to obtain them, which will necessarily require a retest of the perception property needed.

Recommended Background Reading

- [4] Feix, T.; Pawlik, R.; Schmiedmayer, H.; Romero, J. & Kragic, D.: **A Comprehensive Grasp Taxonomy**. In: Robotics, Science and Systems Conference: Workshop on Understanding the Human Hand for Advancing Robotic Manipulation, 2009.
Thorough Analysis of human grasps, also available online at <http://grasp.xief.net/>.
- [13] Jones, L. & Lederman, S.: **Human Hand Function**. Oxford University Press, 2006.
Extensive analysis about the human hand including perception and interaction topics.

References

1. Brownjohn J et al (1980) Errors in mechanical impedance data obtained with impedance heads. *J Sound Vibr* 73(3):461–468. doi:[10.1016/0022-460X\(80\)90527-1](https://doi.org/10.1016/0022-460X(80)90527-1)
2. Bullinger H-J (1978) Einflußfaktoren und Vorgehensweise bei der ergonomischen Arbeitsmitelgestaltung. Universität tuttgart, Habilitation
3. Feix T (2012) Human grasping database. Letzter Abruf. 20.3.2012. <http://grasp.xief.net>
4. Feix T et al (2009) A comprehensive grasp taxonomy. In: Robotics, science and systems conference: workshop on understanding the human hand for advancing robotic manipulation. <http://grasp.xief.net/documents/abstract.pdf>

5. Fu C-Y, Oliver M (2005) Direct measurement of index finger mechanical impedance at low force. In: Eurohaptics conference, and symposium on haptic interfaces for virtual environment and teleoperator systems. World haptics 2005. First joint. Embedded systems and physical science center, Motorola Labs., USA, pp 657–659. doi:[10.1109/WHC.2005.40](https://doi.org/10.1109/WHC.2005.40)
6. Fung Y-C (1993) Biomechanics: mechanical properties of living tissues, 2nd edn. Springer, New York [u.a.], p XVIII, 568. ISBN: 0-387-97947-6, 3-540-97947-6
7. Hajian AZ, Howe RD (1997) Identification of the mechanical impedance at the human finger tip. *J Biomech Eng* 119:109–114. doi:[10.1115/1.2796052](https://doi.org/10.1115/1.2796052)
8. Hannaford B, Anderson R (1988) Experimental and simulation studies of hard contact in force reflecting teleoperation. In: IEEE international conference on robotics and automation, vol 1. Jet Propulsion Lab., Caltech, Pasadena, CA, USA, pp 584–589. doi:[10.1109/ROBOT.1988.12114](https://doi.org/10.1109/ROBOT.1988.12114)
9. Hatzfeld C (2013) Experimentelle analyse der menschlichen Kraftwahrnehmung als ingenieurtechnische Entwurfsgrundlage für haptische Systeme. Dissertation, Technische Universität Darmstadt. <http://tuprints.ulb-tu-darmstadt.de/3392/>. München: Dr. Hut Verlag. ISBN: 978-3-8439-1033-0
10. Hatzfeld C, Neupert C, Werthschützky R (2013) Systematic consideration of haptic perception in the design of task-specific haptic systems. *Biomed Tech* 58. doi:[10.1515/bmt-2013-4227](https://doi.org/10.1515/bmt-2013-4227)
11. Israr A, Choi S, Tan HZ (2006) Detection threshold and mechanical impedance of the hand in a pen-hold posture. In: International conference on intelligent robots and systems (IROS), Peking, pp 472–477. doi:[10.1109/IROS.2006.282353](https://doi.org/10.1109/IROS.2006.282353)
12. Israr A, Choi S, Tan HZ (2007) Mechanical impedance of the hand holding a spherical tool at threshold and suprathreshold stimulation levels. In: Second joint EuroHaptics conference and symposium on Haptic interfaces for virtual environment and teleoperator systems (WorldHaptics conference), Tsukuba. doi:[10.1109/WHC.2007.81](https://doi.org/10.1109/WHC.2007.81)
13. Jones L, Lederman S (2006) Human hand function. Oxford University Press, Oxford. ISBN: 0195173155
14. Jungmann M, Schlaak HF (2002) Taktiles Display mit elektrostatischen Polymeraktoren. In: Konferenzband des 47. Internationalen Wissenschaftlichen Kolloquiums, Technische Universität Ilmenau. <http://tubiblio.ulb-tu-darmstadt.de/17485/>
15. Jungmann M (2004) Entwicklung elektrostatischer Festkörperaktoren mit elastischen Dielektrika für den Einsatz in taktillen Anzeigefeldern. Dissertation, Technische Universität Darmstadt, p 138. <http://tuprints.ulb-tu-darmstadt.de/500/>
16. Kern T et al (2006) Study of the influence of varying diameter and grasp-forces on mechanical impedance for the grasp of cylindrical objects. In: Proceedings of the Eurohaptics conference, Paris. doi:[10.1007/978-3-540-69057-3_21](https://doi.org/10.1007/978-3-540-69057-3_21)
17. Kunstmann C (1999) Handhabungssystem mit optimierter Mensch-Maschine-Schnittstelle für die Mikromontage. VDI-Verlag, Düsseldorf. ISBN: 978-3-642-57024-7
18. Milner TE, Franklin DW (1998) Characterization of multijoint finger stiffness: dependence on finger posture and force direction. *IEEE Trans Biomed Eng* 43(11):1363–1375. doi:[10.1109/10.725333](https://doi.org/10.1109/10.725333)
19. Oguztoreli MN, Stein RB (1990) Optimal task performance of antagonistic muscles. *Biol Cybern* 64(2):87–94. doi:[10.1007/BF02331337](https://doi.org/10.1007/BF02331337)
20. Salisbury C et al (2011) What you can't feel won't hurt you: evaluating haptic hardware using a haptic contrast sensitivity function. *IEEE Trans Haptics* 4(2):134–146. doi:[10.1109/TOH.2011.5](https://doi.org/10.1109/TOH.2011.5)
21. Serina Elaine R, Mote C, Rempel D (1997) Force response of the fingertip pulp to repeated compression—effects of loading rate, loading angle and anthropometry. *J Biomech* 30(10):1035–1040. doi:[10.1016/S0021-9290\(97\)00065-1](https://doi.org/10.1016/S0021-9290(97)00065-1)
22. Wiertelwski M, Hayward V (2012) Mechanical behavior of the fingertip in the range of frequencies and displacements relevant to touch. *J Biomech* 45(11):1869–1874. doi:[10.1016/j.jbiomech.2012.05.045](https://doi.org/10.1016/j.jbiomech.2012.05.045)
23. Yoshikawa T, Ichinoo Y (2003) Impedance identification of human fingers using virtual task environment. In: IEEE/RSJ international conference on intelligent robots and systems (IROS 2003), vol 3, pp 3094–3099. doi:[10.1109/IROS.2003.1249632](https://doi.org/10.1109/IROS.2003.1249632)